Hollow-Core Light Guide and Scintillator Based Near-Core Temperature and Flux Probe

David E. Holcomb, Leon Maya, and Michelle D. Pawel—Oak Ridge National Laboratory
Don W. Miller, Joseph W. Talnagi, and Hanying Liu—The Ohio State University
Michael E. Mickelson—Denison University

Abstract

A miniature, optically based, in-core, self-powered neutron flux and temperature probe has been demonstrated to function in a near-core environment. Optically based measurements are among the most common technologies throughout modern industrial instrumentation architectures. However, operating nuclear power plant measurement chains are almost totally devoid of optical technologies. Because optically based transduction and signal transmission have significant advantages over conventional technologies, future reactors will almost certainly employ optically based sensors. The focus of the current project has been on demonstrating a representative optically based measurement in a near-core environment. Conceptually the new sensor consists of a scintillator and neutron converter assembly located at the distal end of a light guide whose proximal end is located in a benign environment. The scintillator and neutron converter assembly consists of a uranium layer placed against a thick (few microns) scintillator layer. The fission fragments resulting from neutron interactions in the uranium produce light in the scintillator. Simultaneously the temperature of the scintillator results in blackbody type photon emissions. The light from the sensor is guided out from the reactor core region using a hollow-core optical wave guide. The temporal and wavelength characteristics of the light emerging from the wave guide are measured and used to determine the temperature of the scintillator and the neutron flux incident upon the uranium layer.

1. Introduction

The core transduction technologies underlying nuclear power plant (NPP) process parameter measurements were developed in the 1940s–60s before the revolutionary improvements in optical technologies that have occurred over the past few decades. While to a large extent current-generation sensors adequately perform their intended functions, more modern technologies have the possibility of providing improved measurement accuracy, higher reliability, and lower costs. Moreover, all of the Generation IV (GenIV) NPP concepts would operate at significantly higher temperatures than current-generation light-water reactors, thus requiring development of new generation sensing technologies.

The focus of this paper is on describing the developed instrument and its testing apparatus. A more comprehensive paper focusing on theory of operation and measured sensor performance is currently in preparation for submission to *IEEE Transactions on Nuclear Science*. The new sensor was developed under a U.S. Department of Energy Nuclear Energy Research Initiative (NERI) project. The new instrument demonstrates two key optical technologies. First it establishes scintillation measurements in an environment where it has never before been successfully employed. The sensor configuration is shown as Figure 1. Scintillators have not previously been used in-core both due to the combined temperature and radiation effects as well as the difficulty of guiding the resultant light out-of-core. Second, while hollow-core optical fibers are commonly used in situations where light guiding solids absorb too strongly, they have not previously been employed in environments as extreme as a reactor core. As an initial demonstration of capabilities, the developed instrument remains immature, and significant development remains before either scintillators or hollow-core light guides can be deployed in operating NPPs.

2. Background

The higher temperatures of GenIV reactors necessitate different instruments than those used in light-water reactors. While valuable information can be obtained from ex-core instruments, the most accurate flux and temperature profiles are obtained from measurements directly within the core. This is particularly important for monitoring local disturbances such as single flow channel obstruction. In-core distributed point measurements directly improve the assurance of core integrity by immediately indicating a local flux or temperature

excursion. The operation of pebble bed modular reactors with their chaotic pebble motion and consequent non-uniform pebble distribution would be significantly enhanced by direct, point-wise, in-core flux and temperature measurement. Core physics models can be made more accurate and precise with point in-core measurements. This allows higher fuel burnup and more efficient loadings as well as more uniform power distributions that potentially permit a higher overall power rating. More efficient fuel loadings reduce the volume of high-level waste produced from the reactor. Additionally, combining the flux and temperature measurements onto a single probe halves the required amount of in-vessel instrumentation.

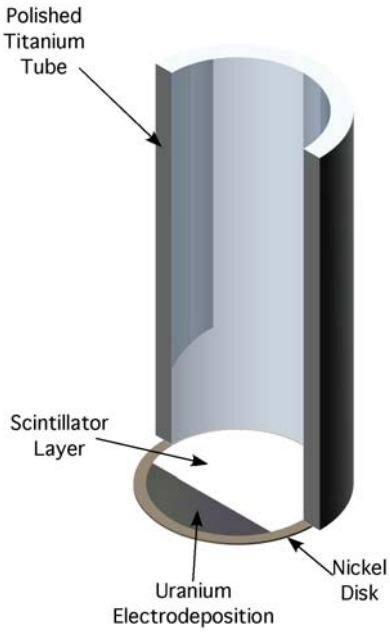

Figure 1— Cut-Away View of Scintillator and Uranium Layers on Nickel Disk at Distal End of Hollow-Core Light Guide Tip

Each of the major project component technologies is based upon well-established prior art. The principal innovation of this project is to combine them in a form suitable for deployment in a nuclear reactor core.

2.1 Hollow-Core Light Guides

No optical measurement electronics will survive in, or near, an operating nuclear reactor core. Therefore, sensor light emission must be guided to the measurement electronics located in a well-controlled, benign environment. Several different implementations can be employed to accomplish this, each with their own advantages and weaknesses. For extreme dose situations, the light must initially be guided from the measurement location using a hollow-core light guide. All known materials darken unacceptably in the intense radiation field of a nuclear reactor core. However, reflective technologies are available that have been shown to withstand comparable environments. [1, 2] Conceptually, a hollow-core light guide is simply a mirror that has been formed into a tube (see Figure 2). Recently single material hollow-core optical fibers (referred to as photonic crystal fibers) have become commercially available. [3, 4] All silica, photonic crystal fibers appear likely to have much larger radiation tolerance than conventional optical fiber technologies.

As the light reaches lower radiation environments, several different optical transmission technologies become possible: (1) hollow-core light guides with relaxed temperature and radiation tolerance (meaning less exotic construction materials); (2) conventional, radiation-tolerant optical fibers; and (3) relay optics (i.e., telescope). Hollow-core light guides for temperatures below 800 K can be constructed of materials more easily processed and coated than high-temperature alloys. [5, 6] For total doses up to about 10^4 Gy, pure silica core, fluorosilica clad, multimode optical fibers are suitable light guides. [7] Relay optics are another alternative for transmitting the light back to the measurement electronics.

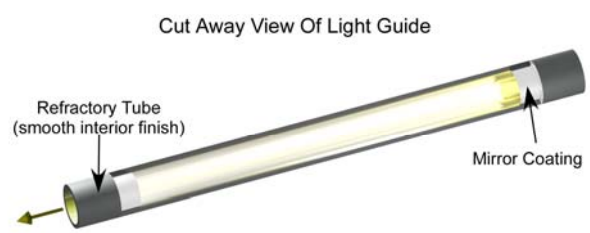

Figure 2—Hollow-Core Light Guide Concept.

2.2 Radiation Thermometry

Radiation thermometry relies upon the variation of temperature-induced light emission from a surface with changes in its temperature. The origin of this surface radiance is the acceleration (vibration) of the atoms within the material. Conservation of momentum dictates that anytime a particle undergoes acceleration, such as the continuous changes in direction of electrons as they orbit nuclei, it must emit a particle with equal and opposing momentum. In the case of nuclei and electrons vibrating with temperature, photons are the emitted particles. This emission inherently takes place continuously from all

materials. Because acceleration of the electrons and nuclei within materials is a direct consequence of temperature, the amount of light generated varies directly with temperature. The increasing magnitude of acceleration with increasing temperature results in both more emitted photons and larger energies on average for those photons. Neighboring atoms in opaque materials efficiently reabsorb the photons emitted by internal atoms. However, externally directed photons with origins near the surface can escape a material. The probability that thermally emitted photons will escape a material's surface is referred to as its emissivity.

2.3 Scintillators

Scintillation-based measurements are among the most common laboratory and field techniques for radiation measurement. Scintillators function by converting absorbed dose into photons. Initially a scintillator's electronic levels are populated in the ground state. Radiation dose excites some of the electrons into higher energy states. The scintillator electrons then return to ground state via photon (and possibly phonon) emission. Both the lifetime of the excited state and the wavelength of the scintillation photons are characteristic of the scintillator material. While radiation damage will eventually degrade the performance of any scintillator, some scintillator materials are known to perform for extended periods of time under intense radiation conditions. A prime example of this is the endurance of color cathode ray tubes over many years of continuous operation.

The phenomena underlying simple inorganic scintillator degradation under irradiation have been studied for many years and are well understood in general terms. [8] As in all radiation damage, scintillator radiation-induced degradation originates from nuclear transmutation, radiolysis, or atomic displacement. High temperatures can both increase the rate of radiation damage and of its healing. The local chemical environment is often a dominant associative trigger for permanent scintillator radiation damage. For example, the sulfides (CaS, ZnS, CdS, etc.) are common scintillator host materials. However, when irradiated in the presence of oxygen or water vapor they rapidly form minimally luminescent sulfates and hydrogen sulfide gas. The refractory oxides (Y_2O_3, Al_2O_3, etc.) are highly chemically stable. Consequently when the bonds between their constituent atoms are broken radiolytically, they are highly likely to reform into the same configuration. Atomic displacement is particularly destructive of long-range ordered structures. Consequently, scintillators for high-radiation environments are often deployed as micron-sized particulate powders that exhibit minimal long-range order.

Many of the same physical properties required for thermographic phosphors are directly applicable to radiation pulse scintillators. High chemical and temperature inertness, mechanical cohesion and surface adhesion, and high light output are important to both applications. However, the differing excitation mechanisms between radiation pulse scintillation and phosphor thermometry produces different optical responses for the same phosphor material as well as yielding a different optimization of phosphor deposition. Phosphor thermometry is typically optically pumped. Scintillator materials respond differently in both wavelength and time to optical as compared to energetic ion (from the uranium fission) excitation. This is due to two principal causes. First, energetic ions can interact directly with inner-shell electrons as compared to optical photons that only interact with outer-shell electrons. Additionally, lasers and energetic ions exhibit different nonlinear phosphor saturation mechanisms either exciting almost all of the available fluorescing atoms over a laser spot or creating extensive transient local structural disorder (pulse height defect) with energetic ions. Moreover, most available thermographic phosphors are in opaque powder form. The micron-scale phosphor particles effectively block the scintillation light, thereby reducing the active scintillation region to the top few tens of nanometers of scintillator material. While this is not a problem for a front-side optically pumped system with its large number of available scintillation photons, scintillator films for neutron converter application need to be thin enough for the energetic daughter ions to reach the film surface and should be as transparent as possible to their own scintillation light.

3. Experimental Methodology and Apparatus

3.1 Uranium Oxide Film Electrodeposition

The neutron converter material can be composed of any composition that has a large fraction of atoms that produce energetic charged particles in response to neutron irradiation. The optimal material choice depends on the temperature and neutron flux environment in which the sensor is to be deployed. For in-core, at-power deployment an atom with a very high neutron absorption cross-section, such as ^{10}B, will result in a sensor that burns out rapidly and has a significant thermal load. Whereas, a sensor based on a lower cross-section isotope, such as ^{14}N, will not have a neutron-induced fluorescence

signal that is readily distinguishable from the competing gamma-induced signal. This project employed both uranium oxide and boron nitride as candidate neutron converter layers. The boron nitride based test pieces were fabricated by punching out the substrate disks from commercial-grade, natural enrichment boron nitride (95% BN; 5% B_2O_3) sheet stock (1.59 mm thick).

The uranium oxide films were electrodeposited onto nickel disks. Nickel was selected as the deposition substrate because of its high temperature tolerance and relatively low activation. The general procedure used for producing the films has been reported in the literature [9] based on this project. The simplest approach to deposit a uranium film appeared to be the utilization of well-established techniques for the bioassay of actinides based on electrodeposition. [10] The amounts of actinides present in samples of those materials are very small so that invisible deposits are produced which allow for high-resolution alpha spectrometric analysis. The electrodeposition of actinides has been conducted in either alkaline or acid media, but the latter has been developed and employed more frequently after finding a set of reliable conditions. [11] In general, the deposition involves the use of ammonium sulfate as electrolyte in a simple electrochemical cell with a detachable plate as the cathode. The plate is used directly for counting and alpha spectrometry. This project extended the procedure used for bioassay to the deposition of larger amounts of uranium and clarified the mechanistic aspects of film formation and composition.

3.2 Phosphor Coating Methodology

A critical step in the sensor development is bonding (adhering) the scintillator to the uranium neutron converter layer. Many different techniques are employed in different situations for phosphor adhesion. [12] These range from electron-beam evaporation, to radio-frequency sputtering, to laser ablation, to chemical bonding. Many of these bonding procedures are specific to the particular phosphor being applied. Developing a separate deposition technique (implementable in a contamination hood) for each phosphor under consideration was judged to be too difficult.

A procedure was developed to deposit phosphors on flat plates based on the well-known technology used to produce coatings on cathode ray tubes. A few modifications had to be made to accommodate the geometry of the substrate and to allow the use of phosphors that are susceptible to hydrolysis such as alkaline earth sulfides or rare earth phosphors.

The typical procedure used for phosphor screen coating, as communicated by Osram Sylvania, involves the use of barium acetate in addition to the water glass component—a concentrated potassium silicate solution. The use of barium acetate was objectionable because of the carbon that would be introduced, so an alternate formulation was chosen based on a patented process. [13]

The final procedure that we employed consists of preparing an aqueous solution containing 1% potassium silicate concentrate (19.7 wt % SiO_2 and the equivalent of 9.4 wt % K_2O) in 0.1 wt % KOH. One fifth of this solution is used to suspend with rapid stirring the appropriate amount of phosphor, typically enough to give a coating of 4 mg/cm^2 (optimally one fission fragment track length in thickness), which is then added to the other four fifths of the liquid already contained in a tube specially designed to hold the plate onto which the phosphor is deposited. The tube and contents are centrifuged at 1600 rpm for 10 min and the supernatant decanted. The plate containing the phosphor is retrieved and baked for 60 min at 120 °C or alternatively dried for ~10 min under a high-intensity heat lamp. Typical resultant films along with their ultraviolet UV-induced scintillation responses are shown as Figure 3.

Once the sample preparation was complete, the center of the disk was punched to a diameter of 11.3 mm to fit the end of the hollow-core light guide, packaged, and shipped to the Ohio State University Research Reactor (OSURR) for testing. Boron nitride samples were phosphor-coated following the same procedure.

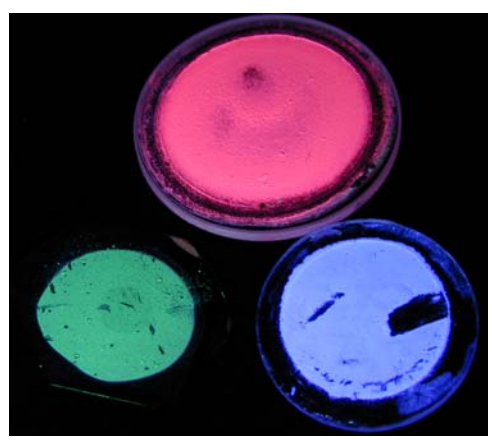

Figure 3—Deposited Scintillation Films: Zinc Sulfide-Silver Activated (Blue), Calcium Sulfide-Cerium Activated (Green), And Magnesium Fluorogermanate-Manganese Activated (Red)

3.3 Light Guide Preparation

The project employed a titanium alloy (3% Al, 2.5% V) with a highly polished interior as the primary light guide. A silvered fused silica tube was deployed above the titanium tube. The titanium alloy tubing had 12.7-mm outer diameter (OD) and 10.2-mm ID. The project applied a standard mechanical metallographic titanium polishing technique to the interior of the light guide and engineered and fabricated the tooling required to implement the polishing on the tubing interior. In brief, first the titanium surface was sanded with 600 grit SiC sandpaper using 35–70 kPa of pressure, followed by progressively finer grit papers. Final polish was implemented using a silk lapping pad with a series of finer and finer (6 μm to 1 μm size) grit diamond polishing slurries. Polished samples are shown in Figure 4.

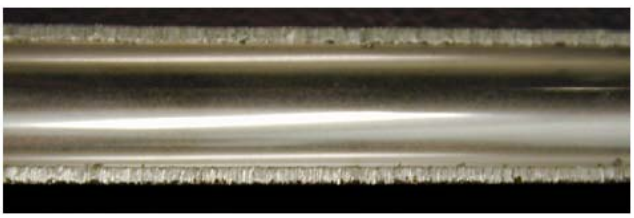

Figure 4—Polished Titanium Tubing Split Open For Examination

3.4 Near-Core High-Temperature Test Assembly

All of the high neutron flux testing was performed using the OSURR. The OSURR is a 19.5% enriched U_3Si_2 fueled, light-water-moderated, pool type research reactor licensed for operation up to 500 kW. [14] The OSURR has several permanent and movable irradiation facilities, including horizontal, 152.4-mm inner-diameter beam tubes, and vertically positioned dry tubes of various diameters. The high-temperature test assembly was fabricated to fit within one of the available, neutral buoyancy, vertical dry tubes. The irradiation tube consists of a continuous 6.1-m-long hollow cylinder of 6021-alloy aluminum with a nominal 101.6-mm OD and 88.9-mm ID. The tube provides sufficient space to accommodate the sensor and heater assembly. Figure 5 shows the facility in its irradiation position.

At full operating power, the high-temperature irradiation tube location receives a total neutron flux of approximately 5×10^{11} neutrons/cm^2/s, and a tissue-equivalent gamma exposure rate of about 500 kGy/h. These measurements scale linearly with reactor power down to about 1% power, when the power history begins to influence the radiation environment because of fission product inventory in the core.

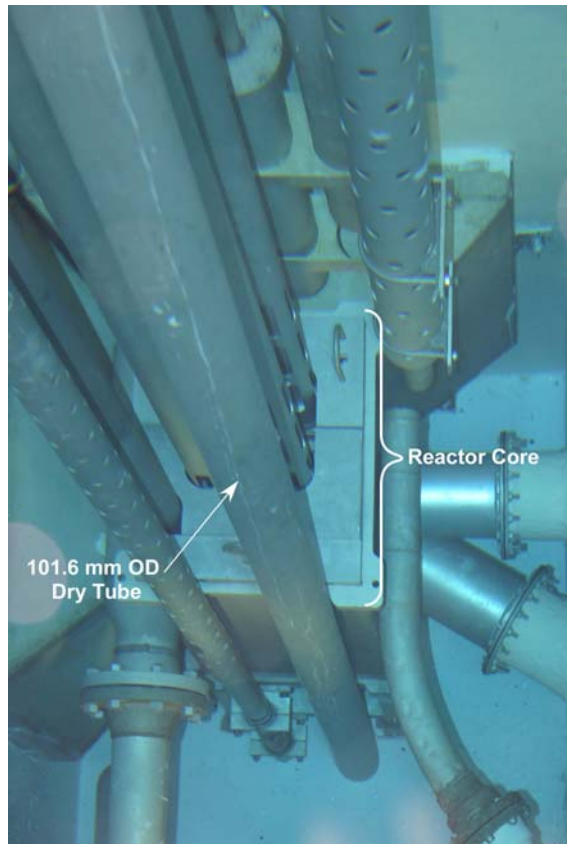

Figure 5—OSURR Dry Tube (Center) In Irradiation Position

The heater assembly is employed to provide a temperature environment designed to emulate an operational environment for higher temperature GenIV power reactor designs. This includes steady-state temperatures greater than 800 °C during sustained operation. To provide this, an insulated tube furnace manufactured by Watlow Electric Manufacturing was selected. [15] This unit features sufficient insulation to provide uniform temperatures along a 305-mm region, and has a central access hole of nominal 25-mm diameter. Its overall diameter is a nominal 76 mm, which allows convenient placement within the dry tube.

The heater unit is placed on an insulating mount, which is positioned within the dry tube with positioning spacers. Mounting rods and spacers also provide radial positioning of the furnace within the 101.6-mm tube, so that the assembly is centered within the 88.9-mm diameter. Vertical mounting rods clamp the assembly in

place, so it cannot move once mounted in the irradiation tube.

3.5 Signal Measurement Optics and Electronics

Samples are located at the lower end of the titanium tube and held in place by a small titanium cap threaded to the end of the titanium light guide, designed for ease of sample exchange. A close-up view of the lower end of the light guide assembly showing the sample holder and furnace top is shown as Figure 6.

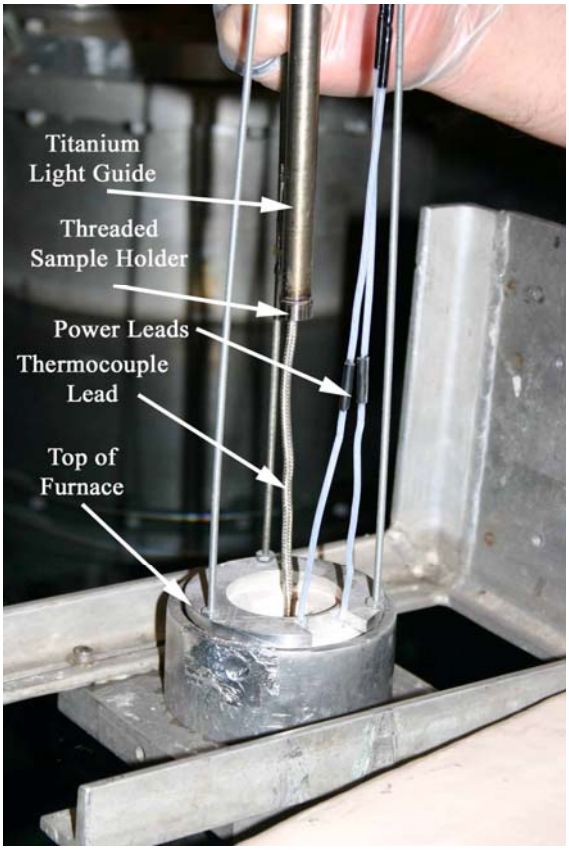

Figure 6—Close Up View of Exterior of Distal End of Light Guide Assembly and Furnace Assembly

Light from the sample was guided up the light pipe assembly to a collimating lens coupled to a 600-µm-diameter optical fiber. The exit end of the optical fiber interfaced with another collimating lens, which directed quasi-parallel light to a Hamamatsu type R192A photomultiplier tube (PMT). A Stanford Research Systems Model SR400 Gated Photon Counter was used to measure light output from the PMT. Data from the analog output of the photon counting system were sent to a computer-based data acquisition system, which used a custom designed LabView™ Virtual Instrument (VI) data acquisition program. In some instances, the optical fiber was connected to an Ocean Optics™ model USB2000 Spectrometer to record the optical spectrum emitted by the scintillator under test in the Optics software on a laptop computer. The wavelength range recorded was approximately 350 to 1100 nm, all of which was employed in the blackbody temperature measurement.

4. Results and Discussion

Temperature measurement with the new probe functioned as anticipated, becoming significantly brighter at higher temperatures and shifting the peak emission to shorter wavelengths as the probe tip temperature was increased. System stability measurements were not performed, nor were the emissivities of the different scintillators compared to establish a calibration. Overall, significantly more measurements must be performed to establish the viability of the present system to make useful temperature measurements under near-core type environments.

A series of disks with different scintillators were prepared and tested for reactor-induced scintillation response. Both boron-10 and uranium-235 were employed as underlying neutron converters. Only representative data from the measurement campaign will be presented here. In a typical reactor run, the reactor power was incremented as follows: 50 kW, 100 kW, 200 kW, 300 kW, 400 kW and 450 kW. Each power level was usually maintained for approximately 5 min. However, in several cases the power level was maintained for somewhat longer to observe any longer term effects on the output of the detector disk. A typical scintillator measured response is shown as Figure 7.

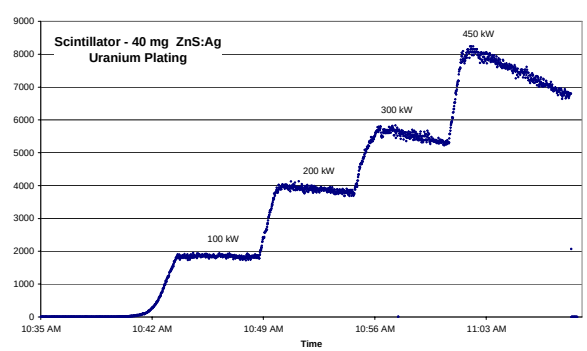

Figure 7—Typical Scintillation Response Curve for ZnS:Ag Scintillator

It is unknown to what extent the scintillation decrease with time at reactor power is due to the rising temperature

of the scintillator. Further testing was performed with the same scintillation disk at a reactor power of 100 kW while allowing the disk to cool from 265 °C to 52 °C over a period of approximately 1 h and 40 min. The results of this measurement are shown as Figure 8.

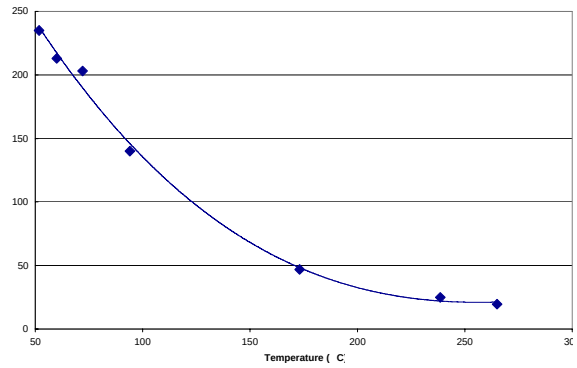

Figure 8—Increase in Scintillation As Disk Cools at Constant Reactor Power

The optical spectrum of the scintillation light transmitted to the Ocean Optics™ spectrometer was also measured (shown in Figure 9). The measurements demonstrate that the characteristic blue glow of ZnS:Ag dies away under reactor irradiation with increasing temperature.

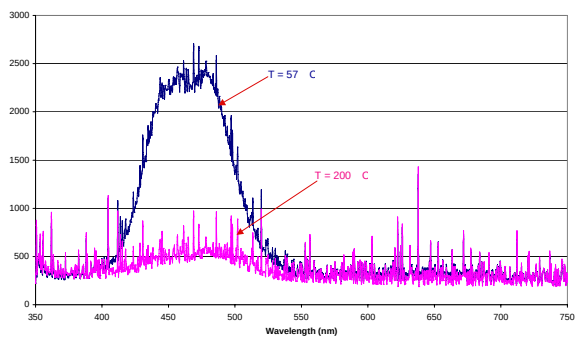

Figure 9—Characteristic Scintillation Decrease With Increasing Temperature at Constant Reactor Power

Another experiment was performed to examine the dynamic response of the same scintillation disk. Figure 10 shows the measured response just before and during the scram. The detector count rate was sampled 10 times/s during the scram. A fit to the sensor response time in the steepest portion of the scram curve was on the order of 0.21 s. A typical value for the reactor response in this portion of the shutdown curve is 0.23 s as measured using an ion chamber.

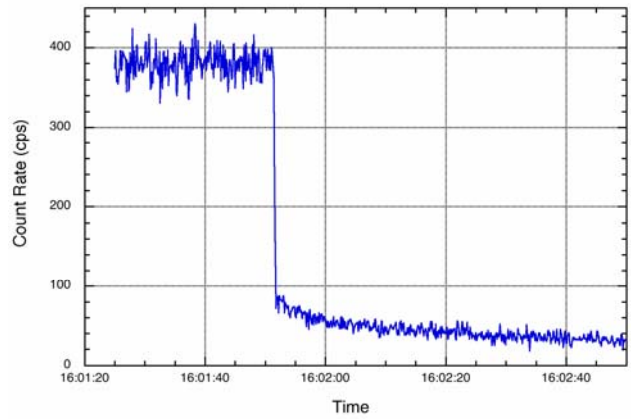

Figure 10—Scram Response of ZnS:Ag on Uranium Scintillation

Similar measurement results were obtained using Y_2O_3:Eu and YAG:Tb scintillators. YAG:Tb is a green scintillator. The photomultiplier response function is somewhat lower for it than the blue ZnS:Ag. The measured YAG:Tb pulse count rate vs reactor power is shown in Figure 11.

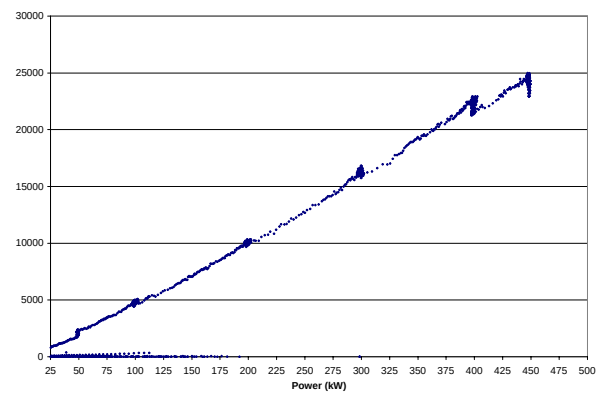

Figure 11—Disk 12/16; YAG:Tb Measured Reactor Induced Scintillation

The YAG:Tb scintillator also exhibited a light output degradation similar to the ZnS:Ag. This is shown in Figure 12.

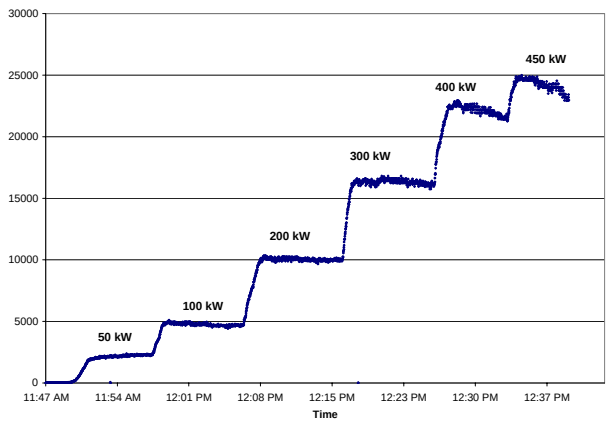

Figure 12—Disk 12/16; YAG:Tb Scintillation Intensity Degradation With Accumulated Reactor Exposure

YAG:Tb is a green-emitting scintillator under optical excitation. It exhibits similar wavelength characteristics under reactor irradiation. The measured optical spectrum is shown in Figure 13.

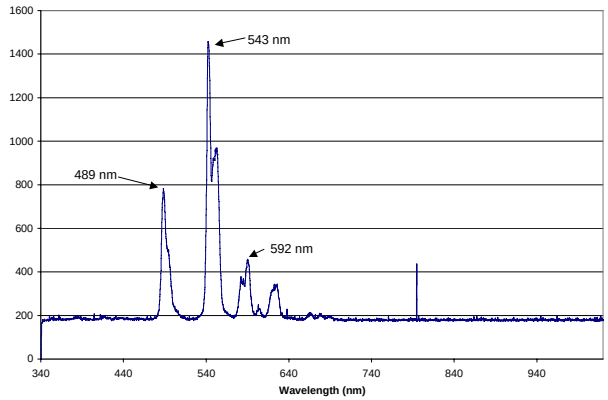

Figure 13—YAG:Tb Reactor Induced Scintillation Spectrum

5. Conclusions

This project has successfully demonstrated the base technologies underlying the application of scintillators and hollow-core light guides to evaluate near-reactor environments.

The general instrument functional conclusions arising out of the measurements were:

1. In general, the scintillation response of the various phosphors is slightly nonlinear with respect to reactor power and temperature.

2. The emitted light intensity decreases notably with time at power. The degradation has both transient and steady state components. It is unclear to what extent this is a temperature phenomenon.

3. The time response of the scintillation detectors is fast relative to reactor power changes.

4. The measured scintillation spectra arising from reactor irradiation closely match that from Xenon lamp excitation.

5. The scintillation intensity varies strongly with temperature, and this may be the most important long-term stability concern for these detectors.

Significant additional development remains before this technology would be useful for power reactor monitoring. First, the light emission of several of the scintillators decreased with time while in-core, at power. This may represent a local heating phenomenon and thus be reversible, or it may represent a more fundamental chemical change. While it appears that much of the decrease in emission intensity recovers following shutdown, this phenomenon requires further investigation. Also, higher optical efficiency refractory metal light guides are recommended for development. Also both the long-term radiation-induced decrease in surface reflectivity and corrosion product buildup on highly polished surfaces has yet to be determined. Finally, while both temperature and reactor power were independently measured with the new sensor, the two signals were not simultaneously analyzed. Compensation for temperature-induced changes in the scintillator performance thus could not be performed.

6. References

1 *K. Obara, A. Ito, et al,* Development of 15-m-long radiation hard periscope for ITER in-vessel viewing, *Fusion Engineering and Design, 42 (1998) pp. 501–509*

2 *V.G. Konovalov, A.F. Bardamid, et al,* On The Problem Of Material For The In-Vessel Mirrors Of Plasma Diagnostics In A Fusion Reactor, *Fusion Engineering and Design, 56–57 (2001), pp. 923–927*

3 *http://www.crystal-fibre.com/products/airguide.shtm*

4 *P. Russell,* Photonic crystal fibers, *Science*, 299, January 2003, pp. 358-362,

5 *Burak Temelkuran, Shandon D. Hart, Gilles Benoit, John D. Joannopoulos, and Yoel Fink,* Wavelength-Scalable Hollow Optical Fibres With Large Photonic Bandgaps For

CO_2 Laser Transmission, *Nature*, *420, 12 December 2002, pp. 650-4*

6 *Takafumi Watanabe, Hajime Hiraga, Yukio Abe, and Mitsunobu Miyagi*, Fabrication of silver hollow nickel waveguides with multiple inner dielectric layers by the outer-coating method, *Optics Letters, 21(20), October 15, 1996, pp. 1670-3*

7 *David E. Holcomb and Don W. Miller*, A comparison of neutron and gamma damage effects on silica glass in a nuclear reactor radiation environment. *Journal of Nuclear Materials, 1993, 203, pp. 136-150*

8 *http://www.ddc-co.com/articles/38%20-%20Phosphor%20Aging.pdf*

9 *L. Maya, B. D. Gonzalez, M. J. Lance, and D. E. Holcomb*, Electrodeposition of uranium dioxide films, *Journal of Radioanalytical and Nuclear Chemistry, 261(3), 605-607 (2004)*

10 *A. Holmes, editor, The determination of radionuclides in materials of biological origin, AERE-R5474, Harwell, England 1967.*

11 *N. A. Talvitie*, Electrodeposition of Actinides for Alpha Spectrometric Determination, *Analytical Chemistry, 44 (1972) pp. 280-3*

12 *S.W. Allison and G. T. Gillies*, Remote thermometry with thermographic phosphors: Instrumentation and applications, *Review of Scientific Instruments, 68(7), July 1997, pp. 2615-2650*

13 *Y. Morita and N. Watanabe*, Process for forming Phosphor Screen, U. S. Patent 4,513,024, Apr. 1985

14 *http://www-nrl.eng.ohio-state.edu/facilities/reactor.html*

15 *http://www.watlow.com/products/heaters/ht_ceram.cfm*